High Performance Position Sensorless Control Using Rotating Voltage Signal Injection in IPMSM

Sungmin Kim, and Seung-Ki Sul
Seoul National University
599 Gwanangno, Gwanak-gu
Seoul, Korea
Tel.: +82-2-880-7991(ext.106)
Fax: +82-2-878-1452
E-Mail: ksmin@eepel.snu.ac.kr / sulsk@plaza.snu.ac.kr
URL: http://eepel.snu.ac.kr

Keywords

«Control of drive», «Permanent magnet motor», «Sensorless control», «Variable speed drive», «Vector control»

Abstract

This paper describes a new position sensorless control method based on the high frequency rotating voltage signal injection to an Interior Permanent Magnet Synchronous Motor (IPMSM) drives. In this method, the rotor position can be directly calculated from four successive sampled current and voltage values. Compared to conventional heterodyning process, the proposed method is simple to implement and appropriate to increase the frequency of the injection signal up to a half PWM switching frequency. Because of the higher frequency injection and no low-pass-filter in demodulation, the control performance can be enhanced conspicuously.

Introduction

To drive Interior Permanent Magnet Synchronous Motor (IPMSM), the rotor position should be detected. In order to get the rotor position, a position sensor like resolver or encoder has been attached to the rotor axis. This position sensor, however, is burdens not only to the overall cost of the drives system, but also to the reliability of the system. Therefore, numerous researches have been published regarding to the position sensorless detection of rotor position in IPMSM. In the IPMSM operation without a position sensor, the saliency of inductance according to the rotor position can be exploited to detect the rotor position instead of the position sensor [1]-[2]. In higher rotating speed region, the rotor position information can be estimated from voltage equations of IPMSM [2]-[4]. By the estimation of back EMF voltage, the rotor position can be attained. Compared to back EMF based position sensorless control method, inductance saliency based methods are advantageous to detect the rotor position at standstill or lower rotating speed [1], [5]-[7].

The inductance saliency based sensorless method uses the characteristics of IPMSM: the spatial inductance distribution is determined by the rotor position because of the inductance saliency [1]. To extract the rotor position information from this inductance saliency, the high frequency voltage signal has been added to the voltage reference of the current regulator. According to the rotor position, the current response due to the injected voltage signal varies, that means that the current values have information related to the rotor position. To get the rotor position information from the current, the current response due to the injected voltage signal has to be analyzed with the high frequency impedance model of IPMSM. In addition to those analysis results, appropriate demodulation methods to extract the meaningful information from the measured currents have been incorporated.

The signal injection sensorless methods are categorized into two groups according to the injected voltage characteristics. The first group is the rotating voltage signal injection in the stationary reference frame regardless of the rotor position [1], and the second group is the pulsating signal injection in the estimated rotating reference frame [5]-[6], [10]-[11]. These sensorless methods have their own characteristics according to the injected signal type. Those affect the rotor position detection performance, and many research results have reported the relationships between sensorless methods and sensorless performance [12]-[19].

Depending on the injected signal type, many demodulation methods to extract the rotor position have been presented. The conventional demodulation processes for both groups have relied on a heterodyning process to extract the position information from the measured stator currents [1], [5]. For the process, the current should be multiplied by cosine and sine function with the estimated rotor angle and, after that, the information of the position can be obtained through the low-pass-filtering. When the injection frequency increased near to Nyquist limit of the sampling frequency, which is usually the PWM switching frequency in the case of double sampling in a switching period, the design of the digital filter and delay due to the filter may result in rapid degradation of the control performance. Recently, in [9] and [10], by taking advantage of the difference of two consecutive samples of the current, a square-wave type pulsating voltage injection method, whose frequency is a half PWM switching frequency, at the estimated rotor reference frame has been represented without the low-pass-filtering in demodulation process.

In this paper, another high frequency signal injection method, where a rotating voltage signal is injected in the stationary reference frame regardless of the rotor position, is introduced. The proposed method keeps the general PWM method and implements the rotating signal injection whose frequency is a half PWM switching frequency. Only band-pass-filtering where the center frequency of the filter is the frequency of the injected signal, two subtractions and/or additions, and one arctangent operation are used without any low-pass-filtering and no multiplication is used to get the rotor position information. While, in the conventional demodulation processes after the complicated heterodyning process, the calculated output is not the position information itself, but the position error information. However, the proposed method is able to extract the position information itself.

Saliency Based Sensorless Methods

IPMSM can be modeled in the stationary reference frame as (1) where v_{dqs}^{s} stands for the stator voltage, i_{dqs}^{s}, the stator current, λ_{dqs}^{s}, a flux linkage in the stationary reference frame, and R_S, stator resistance. A flux linkage in the stationary reference can be expressed with stationary d-/q-axis current as (2) where λ_f stands for the permanent magnet flux linkage, θ_r is rotor position and ΣL and ΔL are related to the d-/q-axis inductance (L_{ds}, L_{qs}) in the synchronous reference as (3). With (2) and (3), the voltage equation in the stationary reference frame can be rewritten as (4).

$$V_{dqs}^{s} = R_s i_{dqs}^{s} + \frac{d}{dt}\lambda_{dqs}^{s} \tag{1}$$

$$\lambda_{dqs}^{s} = \begin{bmatrix} \Sigma L + \Delta L\cos 2\theta_r & \Delta L\sin 2\theta_r \\ \Delta L\sin 2\theta_r & \Sigma L - \Delta L\cos 2\theta_r \end{bmatrix}\begin{bmatrix} i_{ds}^{s} \\ i_{qs}^{s} \end{bmatrix} + \lambda_f \begin{bmatrix} \cos\theta_r \\ \sin\theta_r \end{bmatrix} \tag{2}$$

$$\Sigma L \triangleq \frac{L_{ds} + L_{qs}}{2} \qquad \Delta L \triangleq \frac{L_{ds} - L_{qs}}{2} \tag{3}$$

$$\begin{aligned} V_{dqs}^{s} = {} & R_s i_{dqs}^{s} + \begin{bmatrix} \Sigma L + \Delta L\cos 2\theta_r & \Delta L\sin 2\theta_r \\ \Delta L\sin 2\theta_r & \Sigma L - \Delta L\cos 2\theta_r \end{bmatrix}\frac{d}{dt}\begin{bmatrix} i_{ds}^{s} \\ i_{qs}^{s} \end{bmatrix} \\ & + \omega_r \left\{ 2\Delta L \begin{bmatrix} -\sin 2\theta_r & \cos 2\theta_r \\ \cos 2\theta_r & \sin 2\theta_r \end{bmatrix}\begin{bmatrix} i_{ds}^{s} \\ i_{qs}^{s} \end{bmatrix} + \lambda_f \begin{bmatrix} -\sin\theta_r \\ \cos\theta_r \end{bmatrix} \right\} \end{aligned} \tag{4}$$

In order to consider the only high frequency model of IPMSM, the voltage model of (1) can be rewritten as (5) under the assumption that injection frequency is much higher than the fundamental frequency and voltage drop by stator resistance is negligible. From (5), the relationship between the high frequency injected voltage signal and the current response due to the injected voltage signal can be determined. It can be known that the relationship between the injected voltage and the current response is inductive impedance model. In the inductance matrix, there is the real rotor position information, θ_r. Therefore, the rotor position can be obtained as (5). The current response due to the injected voltage signal can be deduced as (6).

$$V_{dqsh}^{s} = \begin{bmatrix} \Sigma L + \Delta L\cos 2\theta_r & \Delta L\sin 2\theta_r \\ \Delta L\sin 2\theta_r & \Sigma L - \Delta L\cos 2\theta_r \end{bmatrix} \frac{d}{dt} \begin{bmatrix} i_{dsh}^{s} \\ i_{qsh}^{s} \end{bmatrix} \tag{5}$$

$$\begin{bmatrix} i_{dsh}^{s} \\ i_{qsh}^{s} \end{bmatrix} = \int \frac{1}{\Sigma L^2 - \Delta L^2} \begin{bmatrix} \Sigma L - \Delta L\cos 2\theta_r & -\Delta L\sin 2\theta_r \\ -\Delta L\sin 2\theta_r & \Sigma L + \Delta L\cos 2\theta_r \end{bmatrix} \begin{bmatrix} v_{dsh}^{s} \\ v_{qsh}^{s} \end{bmatrix} dt \tag{6}$$

To extract the rotor position related information from (6), the rotating voltage signal in the stationary reference frame can be injected [1]. The injected voltage in the stationary reference frame can be decided as (7) and this voltage signal is rotating spatially as shown in Fig. 1. By substituting (7) to (6), the current response due to the injected voltage signal can be derived as (8). The current response values in (8) have the rotor position related information in the second terms.

$$v_{dqsh}^{s} = \begin{bmatrix} v_{dsh}^{s} \\ v_{qsh}^{s} \end{bmatrix} = V_{inj} \begin{bmatrix} -\sin\omega_h t \\ \cos\omega_h t \end{bmatrix} \tag{7}$$

$$\begin{bmatrix} i_{dsh}^{s} \\ i_{qsh}^{s} \end{bmatrix} = \frac{V_{inj}}{\Sigma L^2 - \Delta L^2} \begin{bmatrix} \frac{\Sigma L}{\omega_h}\cos\omega_h t + \frac{\Delta L}{2\omega_r - \omega_h}\cos(2\theta_r - \omega_h t) \\ \frac{\Sigma L}{\omega_h}\sin\omega_h t + \frac{\Delta L}{2\omega_r - \omega_h}\sin(2\theta_r - \omega_h t) \end{bmatrix} \tag{8}$$

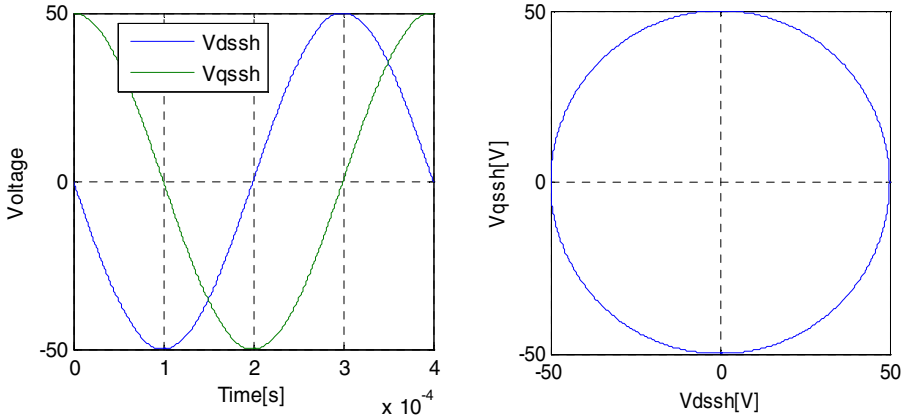

Fig. 1: Injection rotating voltage in the stationary reference frame.

To extract the rotor position information, the demodulation process has to be incorporated. Conventional demodulation methods have used the heterodyning technique as (9). In (9), ε has the rotor position related information. To remove the first term which includes two times injected frequency component in (9), the Low-Pass-Filter (LPF) can be employed. Then the filtered value under the assumption of the perfect cut-off of the high frequency tern, ε_f can be deduced as (10), that is proportional to the rotor position error between the real rotor position and the estimated rotor position.

$$\varepsilon = -i_{dsh}^{s}\sin\left(2\hat{\theta}_r - \omega_h t\right) + i_{qsh}^{s}\cos\left(2\hat{\theta}_r - \omega_h t\right)$$
$$= \frac{-V_{inj}}{\Sigma L^2 - \Delta L^2}\left(\frac{\Sigma L}{\omega_h}\sin 2\left(\hat{\theta}_r - \omega_h t\right) + \frac{\Delta L}{2\omega_r - \omega_h}\sin 2\left(\hat{\theta}_r - \theta_r\right)\right) \tag{9}$$

$$\varepsilon_f \approx \frac{-V_{inj}}{\Sigma L^2 - \Delta L^2}\frac{\Delta L}{\omega_h}\sin 2\left(\theta_r - \hat{\theta}_r\right) \qquad \left(\because \omega_r \ll \omega_h\right)$$
$$\approx \frac{-V_{inj}}{\Sigma L^2 - \Delta L^2}\frac{\Delta L}{\omega_h}2\left(\theta_r - \hat{\theta}_r\right) \triangleq K_e\left(\theta_r - \hat{\theta}_r\right) \qquad \left(\because \theta_r \approx \hat{\theta}_r\right) \tag{10}$$

This conventional demodulation process is shown in Fig. 2 as a signal processing block diagram. The result of demodulation process, ε_f is not the rotor position, but the position error. Therefore, the Luenberger observer or the phase-locked loop state filter should be followed to get the rotor position. The value related to the position error, ε_f, is proportional to the position error by variable constant, K_e as seen from (10), which can be varying according to the operating condition due to the variation of the inductances. Fig. 3 shows the entire control block diagram of the sensorless current control system. Ideally, the injection frequency component of the voltage reference has to be only the voltage comes from the injected voltage signal. To prevent the current controller from generating the injection frequency component in the process of the current regulation, the LPF should be included in current feedback loop in Fig. 3. And the bandwidth of the current regulation loop should be lower than the cut-off frequency of LPF.

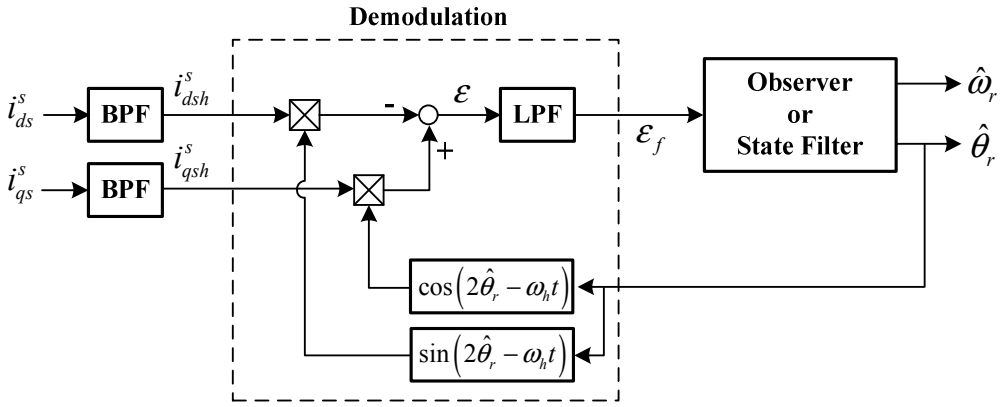

Fig. 2: Control block diagram of conventional demodulation process to extract the rotor position related information.

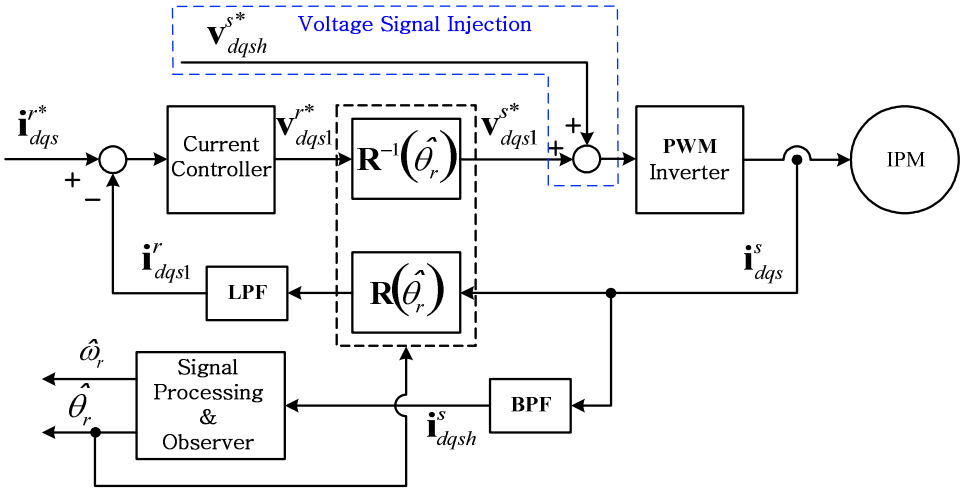

Fig. 3: Entire block diagram of sensorless current control operation.

Rotor Position Extraction Using Half PWM Switching Frequency Signal Injection

In this section, a new modulation method to extract the real rotor position from current response with the half PWM switching frequency rotating voltage signal is proposed. This method is a kind of direct calculation method. Synchronized with PWM carrier signal, the injection voltage signal and current sampling sequence in stationary reference frame is illustrated in Fig. 4. The frequency of the injected voltage signal is a half of the PWM switching frequency and the magnitude of the signal is V_{inj} in Fig. 4. For one period of injected voltage signal, the currents are sampled four times. The sampled currents are called as (i_{dsh1}^r, i_{qsh1}^r) ~ (i_{dsh4}^r, i_{qsh4}^r). Using the Band-Pass-Filter, the injection frequency component of the measured current can be detected. From (8), the sampled currents in the injection frequency can be deduced as (11) ~ (14). By simple addition and subtraction, the sine and cosine function of rotor position can be obtained as (15). By arctangent operation of (15), the real rotor position can be calculated directly continuously with the successive sampled current in every sampling instance. In Fig. 5, the demodulation process of the proposed method is depicted as the signal processing block diagram. In this demodulation process, no LPF is used. This may further enhance the rotor position estimation performance.

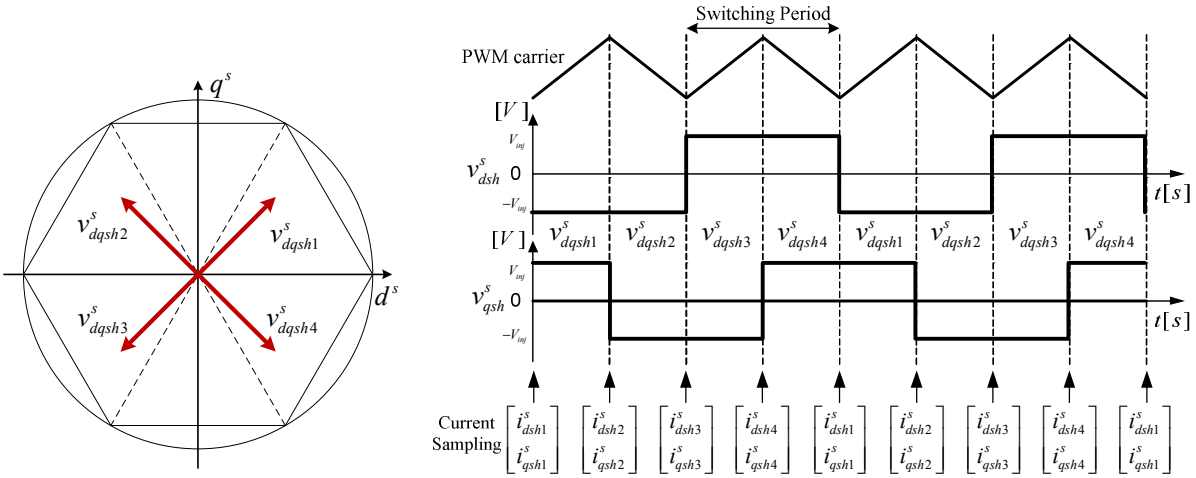

Fig. 4: Signal injection and current sampling sequence in time domain.

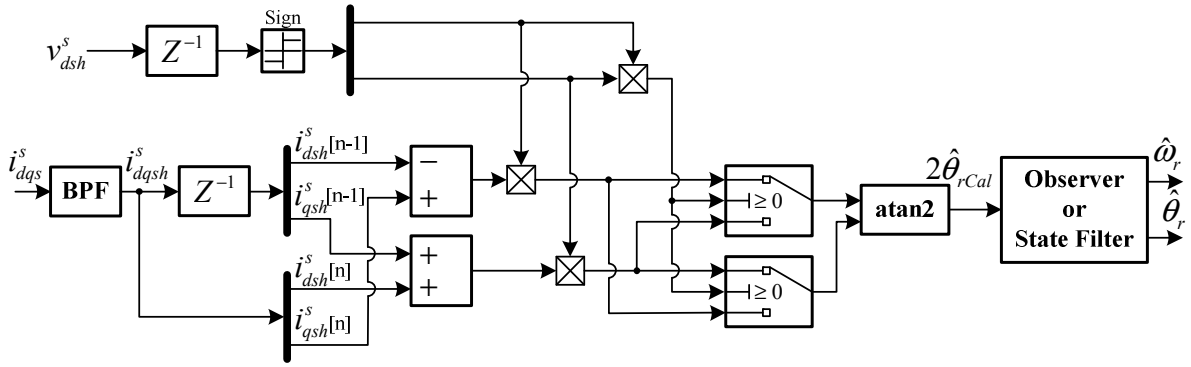

Fig. 5: Implementation of the proposed position sensorless demodulation process

The proposed demodulation method is able to generate two times of the rotor position, and this value has to be inverted to the rotor position, $\hat{\theta}_r$. Generally, Luenberger observer or state filter can be employed to extract more clear position angle. In the sensorless rotor position estimation, the rotor position value can be affected from the sudden current variation, PWM switching current ripple, many non-ideal phenomenon of PWM inverter. The Luenberger observer or state filter can remove the noise signals from the estimated rotor position. The bandwidth of these observer or filter is very critical to

determine the sensorless algorithm performance. In this paper, the modified Luenberger observer is used to suppress the noises and to get the rotor position from two times of the rotor position signal as shown in Fig. 6.

$$\begin{bmatrix} i^s_{dsh1} \\ i^s_{qsh1} \end{bmatrix} = \frac{V_{inj}}{\Sigma L^2 - \Delta L^2} \begin{bmatrix} \frac{\Sigma L}{\omega_h} + \frac{\Delta L}{2\omega_r - \omega_h}\cos(2\theta_r) \\ \frac{\Delta L}{2\omega_r - \omega_h}\sin(2\theta_r) \end{bmatrix} \quad (\text{when } \omega_h t = 0) \tag{11}$$

$$\begin{bmatrix} i^s_{dsh2} \\ i^s_{qsh2} \end{bmatrix} = \frac{V_{inj}}{\Sigma L^2 - \Delta L^2} \begin{bmatrix} \frac{\Delta L}{2\omega_r - \omega_h}\sin(2\theta_r) \\ \frac{\Sigma L}{\omega_h} - \frac{\Delta L}{2\omega_r - \omega_h}\cos(2\theta_r) \end{bmatrix} \quad \left(\text{when } \omega_h t = \frac{1}{2}\pi\right) \tag{12}$$

$$\begin{bmatrix} i^s_{dsh3} \\ i^s_{qsh3} \end{bmatrix} = \frac{V_{inj}}{\Sigma L^2 - \Delta L^2} \begin{bmatrix} -\frac{\Sigma L}{\omega_h} - \frac{\Delta L}{2\omega_r - \omega_h}\cos(2\theta_r) \\ -\frac{\Delta L}{2\omega_r - \omega_h}\sin(2\theta_r) \end{bmatrix} \quad (\text{when } \omega_h t = \pi) \tag{13}$$

$$\begin{bmatrix} i^s_{dsh4} \\ i^s_{qsh4} \end{bmatrix} = \frac{V_{inj}}{\Sigma L^2 - \Delta L^2} \begin{bmatrix} -\frac{\Delta L}{2\omega_r - \omega_h}\sin(2\theta_r) \\ -\frac{\Sigma L}{\omega_h} + \frac{\Delta L}{2\omega_r - \omega_h}\cos(2\theta_r) \end{bmatrix} \quad \left(\text{when } \omega_h t = \frac{3}{2}\pi\right) \tag{14}$$

$$\begin{bmatrix} i^s_{qsh1} + i^s_{dsh2} \\ i^s_{dsh1} - i^s_{qsh2} \end{bmatrix} = \begin{bmatrix} i^s_{dsh2} - i^s_{qsh3} \\ -i^s_{qsh2} - i^s_{dsh3} \end{bmatrix} = \begin{bmatrix} -i^s_{qsh3} - i^s_{dsh4} \\ -i^s_{dsh3} + i^s_{qsh4} \end{bmatrix} = \begin{bmatrix} -i^s_{dsh4} + i^s_{qsh1} \\ i^s_{qsh4} + i^s_{dsh1} \end{bmatrix} = \frac{V_{inj}}{\Sigma L^2 - \Delta L^2} \begin{bmatrix} \frac{\Delta L}{2\omega_r - \omega_h}\sin(2\theta_r) \\ \frac{\Delta L}{2\omega_r - \omega_h}\cos(2\theta_r) \end{bmatrix} \tag{15}$$

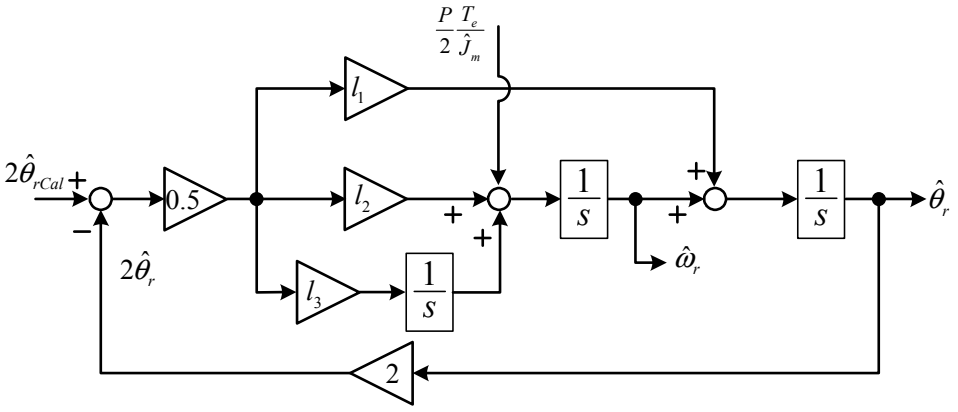

Fig. 6: Implementation of the Luenberger observer for position estimation

Experimental Results

To verify the effectiveness of the proposed method, experimental set-up using to 11kW IPMSM was prepared. The motor parameters and system parameters was listed in Table. I. 10-bit incremental encoder with U, V, W pulses was employed for monitoring purpose. In Fig. 7(a), rotor position, θ_r, is shown with demodulation signal, described as (15). The calculated rotor position tracks the real rotor position well. To verify the sensorless control performance in dynamic situation, the speed control was performed. To get the speed information, a Luenberger observer was used as shown in Fig. 6. The response of the speed control loop for the step speed command from standstill to 300r/min, is shown in Fig. 7(b). Even in the transient state, the position error is less than 0.2rad. In Fig. 7(c), the response of

the loop for the sinusoidal speed command is shown. The magnitude of the speed reference is 100r/min and its frequency is 25Hz. From the figure, the estimated speed tracks the real speed well and the position error is within 0.2rad. Because of the limited pulse number from the encoder in a speed sampling period, the measured speed changes abruptly at near zero speed. While the estimated speed is quite smooth due to the observer. In Fig. 7(d), the sinusoidal speed command with offset speed, 200r/min is shown. Its frequency is 25Hz. The estimated speed tracks the real speed well and the position error is within 0.3rad. And, the response of the position control loop for the sinusoidal position command is demonstrated in Fig. 8. The magnitude of the rotor position command in mechanical angle is +/-2rad and its frequency is 5Hz, and the rotor position error is less than 0.3rad in electrical angle, which means less than 5 degree in mechanical angle.

Table I: IPMSM and system parameters

Rated Power	11 [kW]	Rated current	39.5 [A_{rms}]
Rated Speed	1750 [r/min]	DC-link voltage	310 [V]
Pole Pair	3 (6 pole)	Current sampling frequency	10 [kHz]
Rated Inductance (L_{ds}/L_{qs})	3.4 / 4.6 [mH]	PWM switching frequency	5 [kHz]
Resistance (R_S)	0.104 [Ω]	Injection signal frequency	2.5 [kHz]
PM flux linkage (λ_f)	0.25 [V·s]	Injection voltage	40 [V]

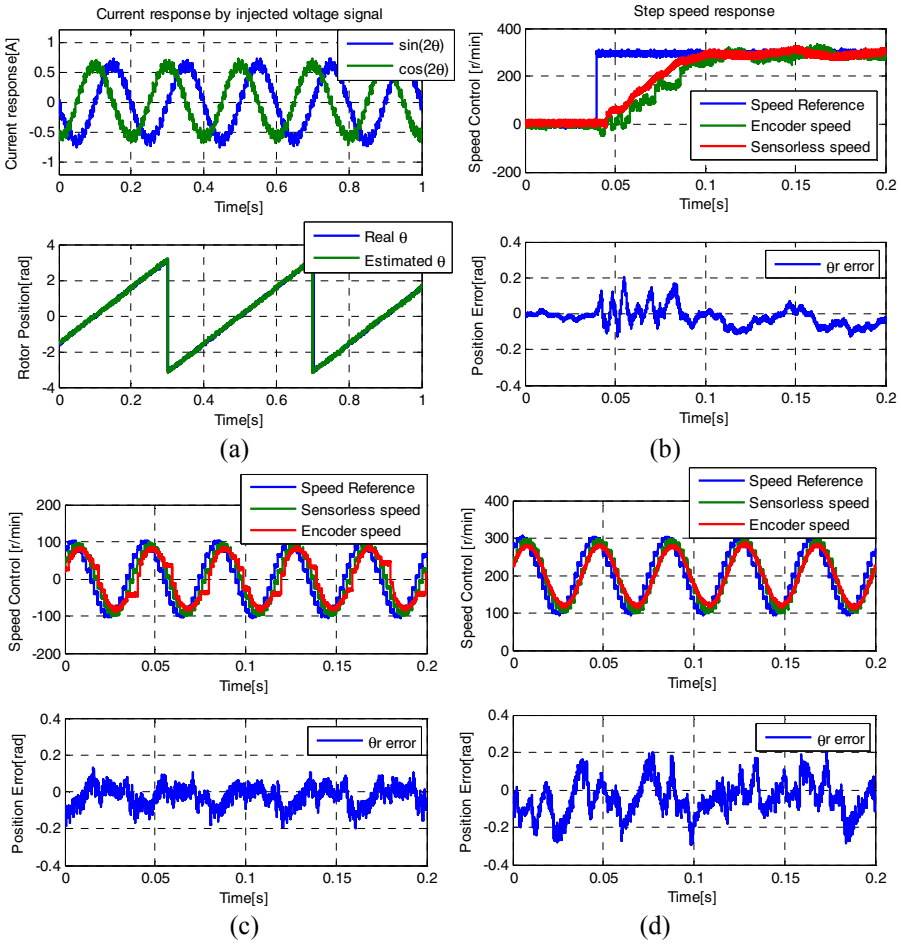

Fig. 7: Experimental results (θ_r calculation, step speed command, sinusoidal speed command and sinusoidal speed command with offset speed) (a) Rotor position by direct calculation (b) Speed control performance with step change (0→300r/min) (c) Speed control performance with the sinusoidal reference (25Hz, 100r/min) (d) Sinusoidal speed control performance with offset speed, 100r/min

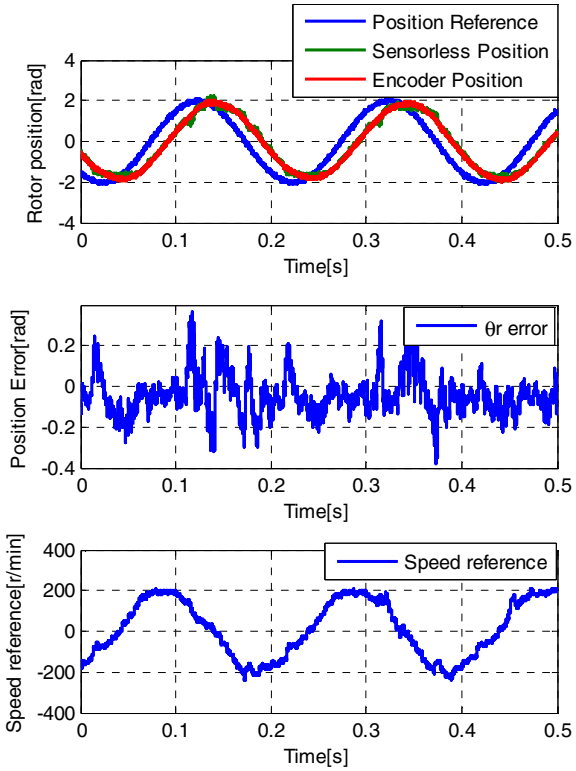

Fig. 8: Sinusoidal position control experimental results (sinusoidal position reference (5Hz / ±2rad): Position reference, sensorless estimated position and encoder position. Position error. Speed reference for position control.

Experiments on a current control mode were performed as shown in Fig. 9. Rotor speed was controlled by load machine, whose speed regulation bandwidth is 5Hz and speed reference is 50r/min. Fig. 9(a), 9(b), and 9(c) show the step response of q-axis current control, zero to 20A, 40A, and 60A, respectively. In the light loaded condition, 20A, that is about 37% of rated load, the position error is less than 0.1 rad. Under the rated load condition, 60A, that is about 110%, the position estimation error is maintained within ±0.6rad.

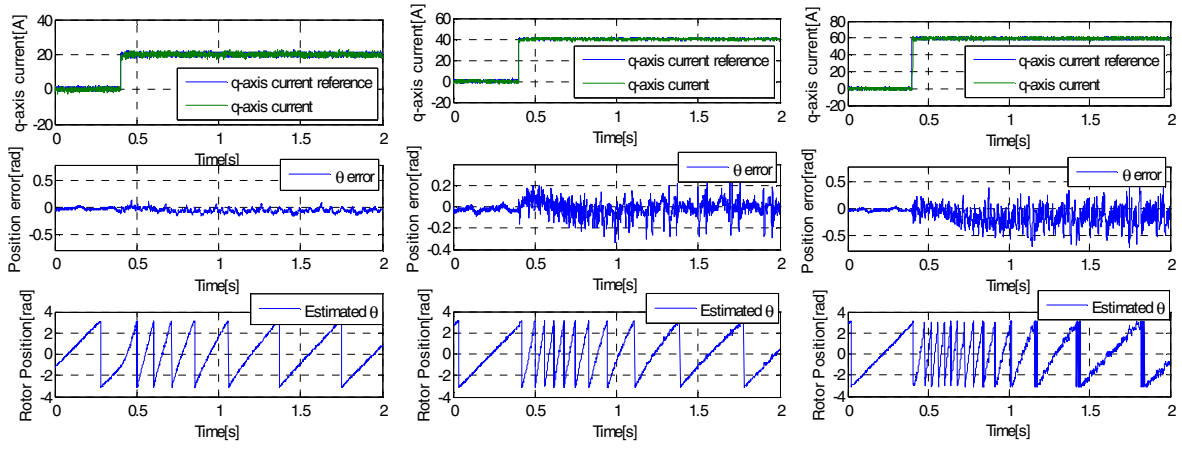

(a) (b) (c)

Fig. 9: Step current control experimental results. (a) q-axis current command: from 0 to 20A(37% rated load). (b) q-axis current command: from 0 to 40A(75% rated load). (c) q-axis current command: from 0 to 60A(110% rated load).

Fig. 10 shows the speed control performance. The step speed command is from 0 to 100r/min and the speed regulation bandwidth is 5Hz. The load condition is 15%, 50%, and 90% in Fig. 10(a), 10(b), and

10(c), respectively. Even though the load is about 90% of rated load, the position estimation error is maintained within ±0.3rad.

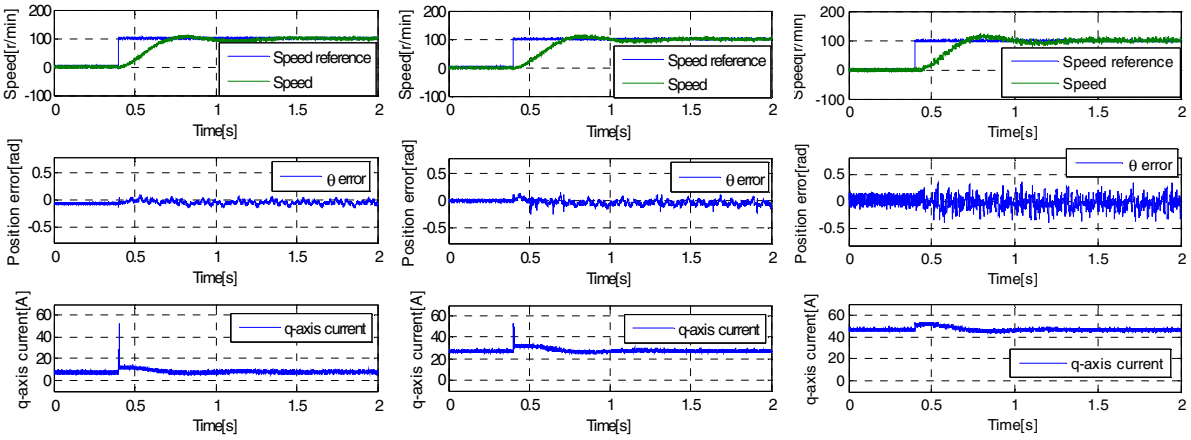

(a) (b) (c)

Fig. 10: Under loaded condition, step speed control experimental results: step speed command from 0 to 100r/min. (a) 15% rated load condition. (b) 50% rated load condition. (c) 90% rated load condition.

Conclusion

In this paper, a position sensorless control method based on a rotating voltage signal injection at the stationary reference frame has been proposed. To improve the performance of sensorless control, the frequency of the injected signal is increased. By increasing the injection frequency up to the half PWM switching frequency, the fundamental frequency is definitely separated from the injection frequency. To overcome the shortcomings of the conventional demodulation process, such as low-pass-filtering and multiplication of the current with sine and cosine of the estimated rotor angle, a direct calculation demodulation method has been devised. This method extracts not the rotor position error, but the real rotor position through two consecutive samples of the current. Even in the transient state, the proposed method can track the real rotor position reasonably well and it does not need any Low-Pass-Filter to extract the rotor position. Through the extensive experimental results, the performance of the proposed method has been verified.

References

[1] P. Jansen, R. Lorenz: Transducerless position and velocity estimation in induction and salient AC machines, IEEE Trans. Ind. Electron., vol. 31, no. 2, pp. 240-247, Mar./Apr. 1995

[2] N. Matsui: Sensorless operation of brushless DC motor drives, IEEE IECON'93, 1993, pp. 739-744

[3] S. Morimoto, K. Kawamoto, M. Sanada, Y. Takeda: Sensorless control strategy for salient-pole PMSM based on extended EMF in rotating reference frame, IEEE Trans. Ind. Appl., vol. 38, no. 4, pp. 1054-1061, Jul./Aug. 2002

[4] B.-H. Bae, S.-K. Sul, J.-H. Kwon, and J.-S. Byeon: Implementation of sensorless vector control for super-high-speed PMSM of turbo-compressor, IEEE Trans. Ind. Appl., vol. 39, no. 3, pp. 811-818, May/Jun. 2003

[5] M. J. Corley, R. D. Lorenz: Rotor position and velocity estimation for a salient-pole permanent magnet synchronous machine at standstill and high speeds, IEEE Trans. Ind. Appl., vol. 34, no. 4, pp. 784-789, Jul./Aug. 1998

[6] J.-I. Ha, S.-K. Sul: Sensorless field-orientation control of an induction machine by high-frequency signal injection, IEEE Trans. Ind. Appl., vol. 35, no. 1, pp. 45-51, Jan./Feb. 1999

[7] M. Schroedl: Sensorless control of AC machine at low speed and standstill based on the 'INFORM' method, IEEE-IAS Annu. Meeting, 1996, pp. 270-277

[8] M. Mamo, K. Ide, M. Sawamura, J. Oyama: Novel rotor position extraction based on carrier frequency component method (CFCM) using two reference frames for IPM drives, IEEE Trans. Ind. Electron., vol. 52, no. 5, pp. 508-514, Apr. 2005

[9] R. Leidhold, P. Mutschler: Improved method for higher dynamics in sensorless position detection, IEEE IECON2008, 2008, pp. 1240-1245

[10] Y.-D. Yoon, S.-K. Sul, S. Morimoto, K. Ide: High bandwidth sensorless algorithm for AC machines based on square-wave type voltage injection, IEEE ECCE2009, 2009, pp. 2123-2130

[11] F. Briz, M. W. Degner, P. Garcia, R. D. Lorenz: Comparison of saliency-based sensorless control techniques for AC machines, IEEE Trans. Ind. Appl., vol. 40, no. 4, pp. 1107-1115, Jul./Aug. 2004

[12] C. Caruana, G. M. Asher, M. Sumner: Performance of HF signal injection techniques for zero-low-frequency vector control of induction machines under sensorless condition, IEEE Trans. Ind. Electron., vol. 53, no. 1, pp. 225-238, Feb. 2006

[13] D. Raca, P. Garcia, D. D. Reigosa, F. Briz, D. L. Lorenz: Carrier-signal selection for sensorless control of PM synchronous machines at zero and very low speed, IEEE Trans. Ind. Appl., vol. 46, no. 1, pp. 167-178, Jan./Feb. 2010

[14] F. Briz, M. W. Degner, A. Diez, R. D. Lorenz: Measuring, modeling, and decoupling of saturation-induced saliencies in carrier-signal injection-based sensorless AC drives, IEEE Trans. Ind. Appl., vol. 37, no. 5, pp. 1356-1364, Sep./Oct. 2001

[15] F. Briz, M. W. Degner, A. Diez, R. D. Lorenz: Static and dynamic behavior of saturation-induced saliencies and their effect on carrier-signal-based sensorless AC drives, IEEE Trans. Ind. Appl., vol. 38, no. 3, pp. 670-678, May/Jun. 2002

[16] J.-I. Ha, K. Ide, T. Sawa, S.-K. Sul: Sensorless rotor position estimation of an interior permanent-magnet motor from initial states, IEEE Trans. Ind. Appl., vol. 39, no. 3, pp. 761-767, May/Jun. 2003

[17] P. Garcia, F. Briz, M. W. Degner, D. D.-Reigosa: Accuracy, bandwidth, and stability limits of carrier-signal-injection-based sensorless control methods, IEEE Trans. Ind. Appl., vol. 43, no. 4, pp. 990-1000, Jul./Aug. 2007

[18] J.-I. Ha: Analysis of inherent magnet position sensors in symmetric AC machines for zero or low speed sensorless drives, IEEE Trans. Magn., vol. 44, no. 12, pp. 4689-4696, Dec. 2008